RF Spatial Modulation Using Antenna Arrays

Zhou, Yijun; Chia, Michael Yan-Wah; Qing, Xianming; Yuan, Jiren

Published in:
IEEE Transactions on Antennas and Propagation

DOI:
10.1109/TAP.2013.2272596

2013

RF Spatial Modulation Using Antenna Arrays

Yijun Zhou, *Member, IEEE*, Michael Yan-Wah Chia, *Senior Member, IEEE*, Xianming Qing, *Member, IEEE*, and Jiren Yuan

***Abstract*—A new method of spatial linear modulation is presented for the RF signal modulation. The constant envelope and phase modulated signals are transmitted to an antenna array and then combined in space; the linear modulation is realized at the same time. The concentric antenna pairs are applied to eliminate the mismatch of phase delay among the modulated signals from different antenna pairs. The measurement results of an RF signal around 2.45 GHz modulated by a 3.84 Mbps QPSK signal are presented. The proposed spatial modulator is able to simplify RF transmitter design and achieve highly efficient power transmission.**

***Index Terms*—Antenna array, linear amplification with nonlinear components (LINC), modulation, outphasing, spatial power combining, wireless.**

I. Introduction

ANTENNA array has been widely applied in beamforming, beam steering, beam-nulling, smart antenna, multiple input multiple output (MIMO) and spatial power combining. Comparing the utilization of an antenna array with that of a single antenna, the former can not only change the beam shape and direction dynamically, but also increase effective isotropic radiated power (EIRP) and signal-to-noise ratio (SNR) for an RF transceiver [1], [2]. Spatial power combiner with antenna array combines power in free-space without loss which occurs in the traditional power combiner, therefore its efficiency is 100% [3]. Spatial power combining is often applied at millimeter-wave frequency due to lack of high power RF devices at this frequency range [3], [4]. Especially with the continually down scaling of CMOS process, spatial power combining provides an effective solution for high power transmission with the low break-down voltage nanometer CMOS circuit, and realizes an antenna-on-chip design [3], [5]. Besides power combining, the spatial modulation with antenna array becomes more interesting in recent years [5]–[10]. Spatial modulation combines RF signals with different phases in free-space, and realizes power combination and RF signal modulation at the same time. Therefore, it can greatly simplify the RF transmitter design and realize the highly efficient power transmission. The previous researches on the spatial modulation were more focused on the directional modulation and secret communication [5]–[10]. This paper presents a novel spatial modulation method which leads to general applications. The proposed method can reduce the complexity and power consumption of an RF transmitter.

A spatial modulator prototype operating around 2.45 GHz and modulated with a 3.84 Mbps QPSK signal is implemented. The distortion analysis and measurement results are provided. This paper is organized as follows. In Section II, the principle for spatial modulation and the architecture of the antenna array are introduced. In Section III, the measurement results are presented and discussed. Finally, the conclusion is given in Section IV.

Manuscript received December 30, 2011; revised February 18, 2013; accepted June 03, 2013. Date of publication July 10, 2013; date of current version October 02, 2013.

Y. Zhou, M. Y.-W. Chia, and X. Qing are with the Institute for Infocomm Research, A*Star, Singapore 138632, Singapore (e-mail: yjzhou@i2r.a-star.edu.sg; chiamichael@i2r.a-star.edu.sg; qingxm@i2r.a-star.edu.sg).

J. Yuan (*retired*) was with the Department of Electrical and Information Technology, Lund University, 221 00 Lund, Sweden (e-mail: jiren.yuan@eit.lth.se).

Digital Object Identifier 10.1109/TAP.2013.2272596

II. Principle for Spatial Modulation

A. Vector Signal Combination

The idea of using outphasing amplifier to generate linear modulation signal was originated from Chireix in the 1930s, and was expanded by Donald C. Cox in the 1970s [11], [12], using an acronym of LINC, Linear Amplification with Nonlinear Components. The architecture and principle of the outphasing amplifier are illustrated in Fig. 1(a) and (b). Linear signal S(t) is combined with two respective constant envelope signals $\mathrm{S_1(t)}$ and $\mathrm{S_2(t)}$

$$S(t) = E(t)\cos[\omega_c t + \phi(t)] \tag{1}$$

$$S_1(t) = E_{\max}\cos[\omega_c t + \phi(t) + \alpha(t)] \tag{2}$$

$$S_2(t) = E_{\max}\cos[\omega_c t + \phi(t) - \alpha(t)] \tag{3}$$

where $S(t) = [S_1(t) + S_2(t)]/2$ and $\alpha(t) = cos^{-1}(E(t)/E_{\max})$.

Since $\mathrm{S_1(t)}$ and $\mathrm{S_2(t)}$ are constant envelope signals, they can be amplified by highly efficient nonlinear amplifiers. The constant envelope signals $\mathrm{S_1(t)}$ and $\mathrm{S_2(t)}$ occupy a larger bandwidth than the original signal S(t) [15]. The linearity of the combined output $\mathrm{S_{out}(t)}$ is determined by the gain and phase match performance of the two amplification channels. Any mismatch between the two amplification channels will cause distortion in the combined signal. To ease the stringent match requirement, the alternating and outphasing modulator (AOM) was developed [13]. Architecture of AOM is shown in Fig. 2. Compared with the architecture of LINC, outphasing signals $\mathrm{S_1(t)}$ and $\mathrm{S_2(t)}$ are alternated between the two amplification channels, thus two new constant envelope signals $\mathrm{S_3(t)}$ and $\mathrm{S_4(t)}$ are generated and amplified to get $\mathrm{S_5(t)}$ and $\mathrm{S_6(t)}$ [13]

$$S_5(t) = GE_{\max}\cos[\omega_c t + \phi(t) + sw(t)\alpha(t)] \tag{4}$$

$$S_6(t) = GE_{\max}\cos[\omega_c t + \phi(t) - sw(t)\alpha(t)] \tag{5}$$

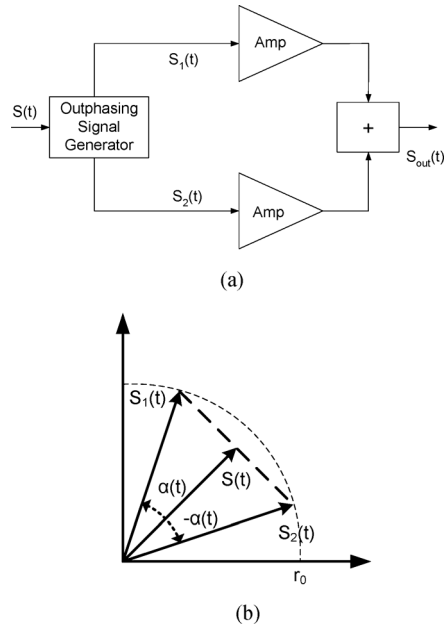

Fig. 1. (a) Outphasing amplifier architecture. (b) Signals in the outphasing amplifier.

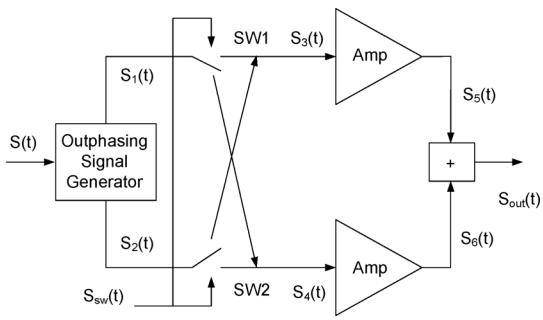

Fig. 2. Architecture of AOM.

where G is the gain of the amplifier, and sw(t) is a square wave signal with amplitude ± 1, angle frequency $\omega_{\rm sw}$ [13]

$$\mathrm{sw(t)} = \sum_{n=1}^{\infty} \mathrm{A_n} \cos(n\omega_{sw} t) \tag{6}$$

$$\mathrm{A_n} = \frac{\sin\left(\frac{n\pi}{2}\right)}{\frac{n\pi}{4}} \tag{7}$$

In Figs. 1 and 2, the constant envelope signals are amplified with nonlinear high efficiency amplifiers and combined with a passive combiner [13]–[15]. Therefore, the efficiencies of LINC and AOM depend on not only the amplifier efficiency, but also the combiner efficiency. The efficiencies of LINC [15] and AOM can be expressed as

$$\eta = \eta_{\rm amp} \cdot \eta_{\rm comb} \tag{8}$$

where η is the efficiency of LINC or AOM, $\eta_{\rm amp}$ and $\eta_{\rm comb}$ are the efficiencies of amplifier and combiner respectively. Both isolated and nonisolated combiners can realize power combination [14]–[17]. The Wilkinson combiner is usually applied as the isolated combiner since it has the advantage of high isolation. According to Fig. 1(b), the linear signal generation is realized by

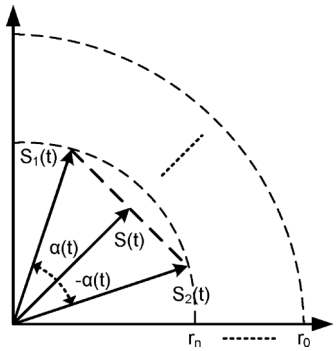

Fig. 3. Signals in the multi-level LINC amplifier.

varying $\alpha(t)$. The in-phase signal components are added in the output and the out-of-phase signal components are dissipated in the isolation load of the isolated combiner. The combiner efficiency can be expressed as [15]

$$\eta_{\rm comb} = \cos^2(\alpha(t)) \tag{9}$$

and the average efficiency $\eta_{\rm avg}$ of LINC is [15]

$$\eta_{\rm avg} = \eta_{\rm amp} \cdot \int_0^{\pi/2} p(\alpha) \cos^2(\alpha) d\alpha \tag{10}$$

where the $p(\alpha)$ is the probability distribution function (PDF) of the signal at $\alpha(t)$. In order to increase the average efficiency of LINC, the multi-level LINC is developed and shown in Fig. 3 [19]. With multiple constant envelop signals, the PDF of α *(t)* in large value is reduced, thus the average efficiency can be increased. The Chireix combiner is a kind of nonisolated combiner, which has higher average efficiency compared with the isolation combiner, but the interaction between the amplifiers degrades the linearity of the combined signal [14], [15].

Besides the passive combiner, the spatial power combining has been widely used for RF signals addition in space [3], [4]. Compared to the passive combiner, the spatial power combiner features the advantages of lower loss and less interaction between the amplifiers. It is especially suitable for multi-source combination at millimeter-wave frequency [3], [4]. However, in the conventional spatial power combiner for linear signal transmission, the linear modulation signal is fed to each antenna, and these signals are combined in space. For the linear signal transmission, power back-off is required for each antenna to achieve linearity [10]. Since the efficiency of the power back-off linear amplifier is low, the efficiency of the conventional spatial power combining architecture is limited. Besides power combination, the spatial directional modulation has been studied as well in recent years [5]–[10]. Fig. 4 depicts the principle of the spatial directional modulation. A constant envelope RF signal is modulated by the phase modulators, and the phase modulated RF signals are combined in space to realize the linear modulation [7]–[10]. With vector signal addition, the spatial directional modulation realizes power combination and linear modulation at the same time, and the high efficiency switch mode power amplifier can be used in each antenna. Therefore, the efficiency of spatial modulation is greatly improved compared to the traditional spatial power combiner.

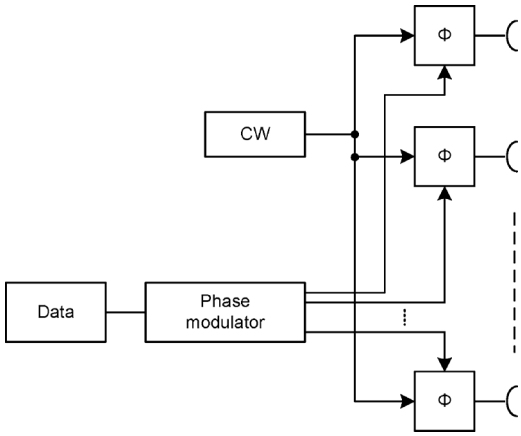

Fig. 4. Architecture of the spatial directional modulation.

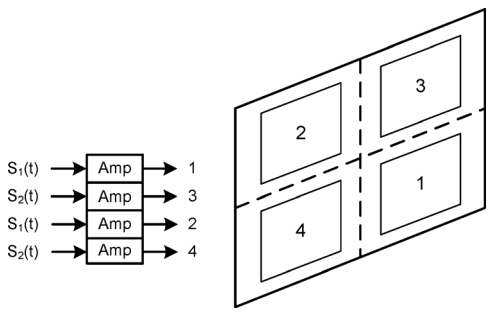

Fig. 5. One implementation of the proposed spatial modulator.

According to the previous researches, there are rigorous requirement of gain and phase match to meet for generating a linear modulation signal based on vector addition [10], [13]–[15], [17]. Thus, the spatial directional modulation can combine vector signals correctly at the specific direction, while at other directions, the combined signals are useless. This feature is well suitable for secret communication, but certainly does not work for general application as the adjacent channel interference is increased due to different phase delay. The motivation for this work is to explore the usage of spatial vector addition with constant envelop signal, realize linear modulation and reduce adjacent channel interference within a wider radial angle.

B. Proposed Spatial Modulator

One of the proposed spatial modulation architectures is shown in Fig. 5. It consists of two concentric antenna pairs, which are connected to the LINC or AOM signals. The amplified LINC or AOM signals are combined in the space instead of the passive combiner to realize the linear modulation. An example of the two concentric antenna pairs is described in Fig. 6. The four isotropic antenna elements are symmetrically positioned in the x-y plane along a circle with a diameter of 2 a. The normalized field of the isotropic antenna element can be written as [18]

$$E_n(r,\theta,\phi) = I_n \frac{e^{-jkR_n}}{R_n} \tag{11}$$

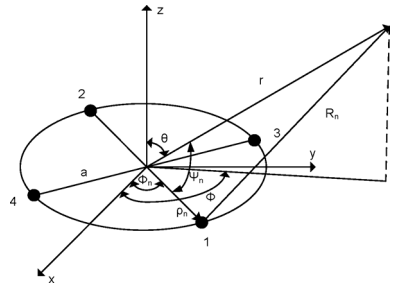

Fig. 6. Concentric antenna pairs.

where R_n is the distance from the nth element to the receiving point, and I_n is the excitation coefficient of n th element. When $r >> a$,

$$R_n \approx r - a\cos\psi_n = r - a\sin\theta\cos(\phi-\phi_n). \tag{12}$$

Assuming that $R_n \approx r$ for amplitude variation, and $I_n = E_0$, (11) can be expressed as [18]

$$E_n(r,\theta,\phi) = \frac{e^{-jkr}}{r} E_0 e^{jka\sin\theta\cos(\phi-\phi_n)}. \tag{13}$$

The combined fields of isotropic element 1 and 2, and element 3 and 4 are

$$\begin{aligned} E_{1+2}(r,\theta,\phi) &= E_1(r,\theta,\phi) + E_2(r,\theta,\phi) \\ &= E_0\frac{e^{-jkr}}{r}(e^{jka\ \sin\ \theta\ \cos(\phi-\phi_1)} \\ &\quad + e^{jka\ \sin\ \theta\ \cos(\phi-(\phi_1+\pi))}) \\ &= E_0\frac{e^{-jkr}}{r}\cdot 2\cos(ka\ sin\,\theta\cos(\phi-\phi_1)) \end{aligned} \tag{14}$$

$$\begin{aligned} E_{3+4}(r,\theta,\phi) &= E_3(r,\theta,\phi) + E_4(r,\theta,\phi) \\ &= E_0\frac{e^{-jkr}}{r}(e^{jka\ \sin\ \theta\ \cos(\phi-\phi_3)} \\ &\quad + e^{jka\ \sin\ \theta\ \cos(\phi-(\phi_3+\pi))}) \\ &= E_0\frac{e^{-jkr}}{r}\cdot 2\cos(ka\ sin\,\theta\cos(\phi-\phi_3)). \end{aligned} \tag{15}$$

From (14) and (15), each concentric antenna pair equalizes with an isotropic element in the centre of the circle. Thus, combined $E_{1+2}(r,\theta,\phi)$ and $E_{3+4}(r,\theta,\phi)$ have the same phase delay but different array factors. The combined array factor depends on θ, and when $\theta = 0$, the two concentric antenna pairs are identical. The difference of array factors between $E_{1+2}(r,\theta,\phi)$ and $E_{3+4}(r,\theta,\phi)$ is reduced with the decrease of θ.

C. Distortion Analysis

In (14) and (15), the combined $E_{1+2}(r,\theta,\phi)$ and $E_{3+4}(r,\theta,\phi)$ have different array factors $2\cos(ka\ \sin\theta\cos(\phi-\phi_1))$ and $2\cos(ka\ \sin\theta\cos(\phi-\phi_3))$ respectively. Since the linearity of LINC and the mixed components level of AOM are determined by the match up of the phase and the gain between the transmission channels, it is important to keep the gain and phase match in the transmission direction. The two antenna pairs have the same phase delay, thus the phase is matched. But the different array factor between the two antenna pairs contributes to the distortion of

the combined signal. The linearity of LINC and the mixed components level of AOM with gain and phase mismatch in the transmission channels are analyzed below. In Fig. 1, LINC architecture, assuming there is a gain mismatch Δ_G between the two amplifier branches, the combined signal is

$$\begin{aligned} S_{out} &= GS_1(t) + (G+\Delta_G)S_2(t) \\ &= GE_{\max}\cos[\omega_c t + \phi(t) + \alpha(t)] \\ &\quad + (G+\Delta_G)E_{\max}\cos[\omega_c t + \phi(t) - \alpha(t)] \\ &= 2GS(t) + \Delta_G E_{\max}\cos[\omega_c t + \phi(t) - \alpha(t)]. \end{aligned} \quad (16)$$

Assuming there is phase mismatch Δ_θ between the two amplifier branches, when $\Delta_\theta << 2\pi$, the combined signal is

$$\begin{aligned} S_{out} &= GS_1(t) + GS_2(t) \\ &= GE_{\max}\cos[\omega_c t + \phi(t) + \alpha(t)] \\ &\quad + GE_{\max}\cos[\omega_c t + \phi(t) - \alpha(t) + \Delta_\theta] \\ &\approx 2GS(t) - \Delta_\theta GE_{\max}\sin[\omega_c t + \phi(t) - \alpha(t)]. \end{aligned} \quad (17)$$

In Fig. 2, AOM architecture, assuming there are gain mismatch Δ_G and phase mismatch Δ_θ between the two amplifier branches, and according to (4)

$$S_5(t) = (G+\Delta_G)E_{\max}\cos[\omega_c t + \phi(t) + \Delta_\theta + sw(t)\alpha(t)]. \quad (18)$$

Combined with $\mathrm{S_6(t)}$ in (5) and the output is [13]

$$\begin{aligned} S_{out}(t) &= S_5(t) + S_6(t) \\ &= r_1\cos[\omega_c t + \phi(t) + \beta_1]\cos[\alpha(t)] \\ &\quad - r_2\sin[\omega_c t + \phi(t) + \beta_2] \\ &\quad \times \sin[\alpha(t)]\sum_{n=1}^{\infty}\mathrm{A_n}\cos(n\omega_{sw}t) \end{aligned} \quad (19)$$

where

$$r_1 = E_{\max}\sqrt{[(G+\Delta_G)\cos(\Delta_\theta)+G]^2+[(G+\Delta_G)\sin(\Delta_\theta)]^2} \quad (20)$$

$$r_2 = E_{\max}\sqrt{[(G+\Delta_G)\cos(\Delta_\theta)-G]^2+[(G+\Delta_G)\sin(\Delta_\theta)]^2} \quad (21)$$

$$\beta_1 = arctg\left(\frac{(G+\Delta_G)\sin(\Delta_\theta)}{(G+\Delta_G)\cos(\Delta_\theta)+G}\right) \quad (22)$$

$$\beta_2 = arctg\left(\frac{(G+\Delta_G)\sin(\Delta_\theta)}{(G+\Delta_G)\cos(\Delta_\theta)-G}\right). \quad (23)$$

In summary, the distortion signals of LINC and AOM due to gain mismatch Δ_G and phase mismatch Δ_θ are described in (16), (17) and (19) respectively. In order to investigate the distortion effects of Δ_G and Δ_θ, two special cases are studied below. When Δ_G and Δ_θ have same percentage variations related to the gain of the amplifier and the period of the RF signal respectively.

Case 1) The gain mismatch between both channels is 10 percent of the channel gain, i.e., $\Delta_G = 10\% \times G$, and the time skew between them is zero, i.e., $\Delta_\theta = 0$.

Case 2) The gains of both channels are equal each other, i.e., $\Delta_G = 0$, and the time skew between them is 10% of a period of the RF signal, i.e., $\Delta_\theta = 10\% \times 2\pi$.

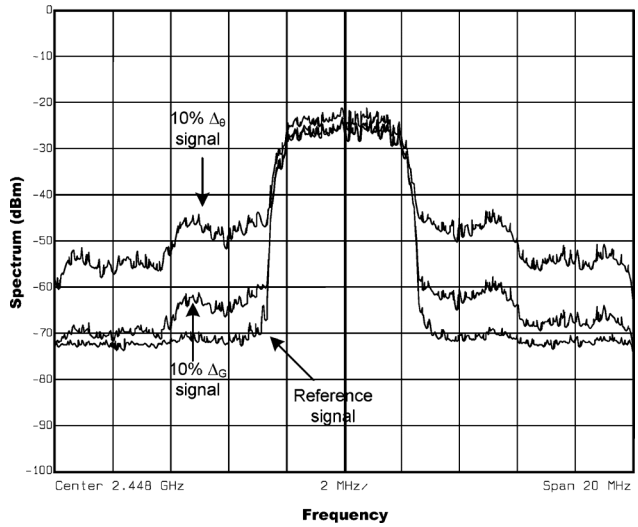

Fig. 7. Measured results of the combined output of LINC architecture.

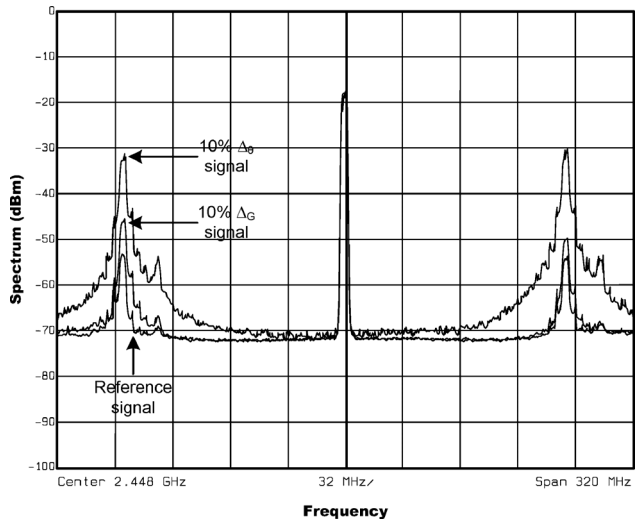

Fig. 8. Measured results of the combined output of AOM architecture.

In the LINC amplifier, according to (16), the amplitude of the distortion signal, $\Delta_G E_{\max}$, is $0.1GE_{\max}$ in Case 1, and according to (17), the amplitude of the distortion signal, $\Delta_\theta GE_{\max}$, is $0.2\pi GE_{max}$ in Case 2 respectively. Thus, the phase mismatch causes more serious distortion compared with the gain mismatch when the same percentage variation happened in the amplitude and phase. In addition, the distortion caused by the phase mismatch is frequency dependent. When the RF frequency increases, the period of the RF signal is shorter, and the distortion contributed by the same amount of the delay mismatch will increase. In contrast, as shown in (16), the distortion level due to the mismatch of the gain does not relate to frequency of the RF signal.

In the AOM architecture, the combined signal with distortion is described in (19). The combined signal consists of S(t) and the mixed components of ω_c and ω_{sw}, and the amplitude of the mixed components is $r_2 A_n sin[\alpha(t)]$. From (21), when there is only gain mismatch Δ_G in the two antenna pairs, i.e., for case 1, $\Delta_\theta = 0$

$$r_2 = \Delta_G E_{\max} \quad (24)$$

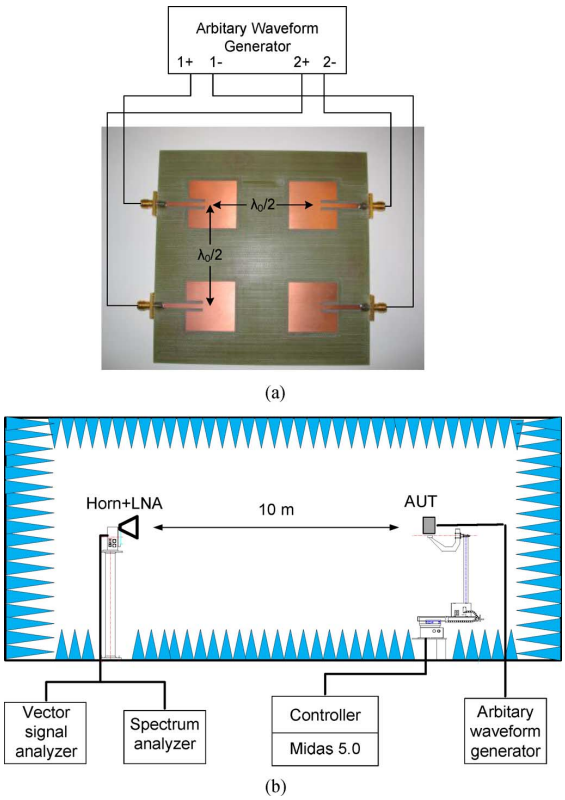

Fig. 9. Antenna array and measurement setup. (a) Antenna array. (b) Measurement setup.

and when there is only phase mismatch Δ_θ in the two antenna pairs, i.e., for case 2, $\Delta_G = 0$, and $\Delta_\theta << 2\pi$

$$r_2 = 2GE_{\max} \sin\left(\frac{\Delta_\theta}{2}\right) \approx \Delta_\theta G E_{\max}. \tag{25}$$

Compared (24) with (16), and (25) with (17), Δ_G and Δ_θ have the similar effect in either AOM or LINC architecture, Δ_θ causes more severe distortions, and the experiment results validate above analysis. Figs. 7 and 8 show the measurement results of LINC and AOM architecture with Case 1, Case 2 and the reference signal, i.e., when $\Delta_G = 0$ and $\Delta_\theta = 0$. In the measurement, an arbitrary waveform generator (AWG) generates two RF signals which are modulated with a 3.84 Mbps QPSK signal through LINC and AOM modulation respectively. The amplitude and time skew are tuned to simulate the variation of Δ_G and Δ_θ, and the two output signals are combined with a commercial power combiner [22].

From Figs. 7 and 8, it shows that AOM has better linearity compared to LINC as the distortion only affects the mixed components level. These results agree with (16), (17) and (19) as stated earlier. However, the AOM architecture is more complicated, and the mixed components should be further reduced with a filter combined with the antenna, or with a band pass function antenna [20], [21]. The LINC architecture is simpler. With the multilevel modulation, the adjacent channel interference can be reduced and the average efficiency of outphasing amplifier can be improved [19]. From (16), (17), (24) and (25), the distortion level of LINC or the mixed components level of AOM is related

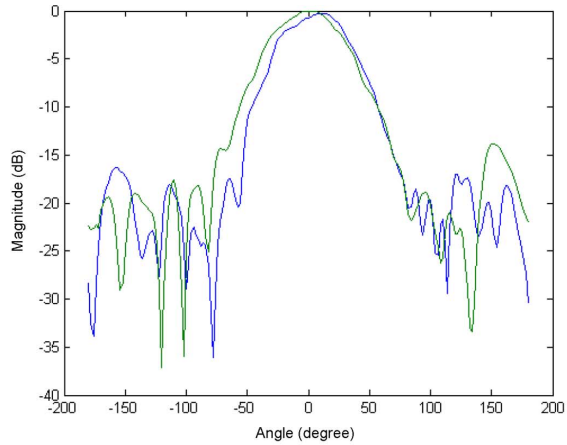

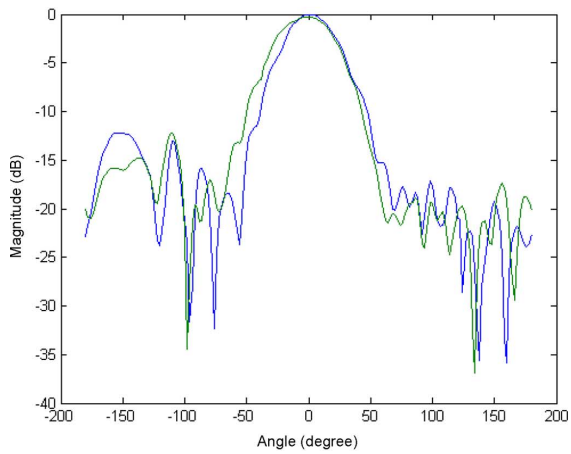

Fig. 10. Radiation patterns of each concentric antenna pair in (a) E-plane. (b) H-plane.

to $E_{\max}$. Therefore, the multilevel modulation can not only improve the average efficiency, but also reduce the distortion of the outphasing amplifier or the mixed components amplitude of AOM.

In the proposed architecture, the concentric antenna pairs are capable to keep the same phase delay among different pairs of antenna arrays to minimize distortion of the outphasing modulation or the level of mixed components of AOM. Furthermore, architecture of the concentric antenna array with multilevel modulation reduces the distortion of LINC or the level of mixed components of AOM due to the phase and the gain mismatch. Consequently, both efficiency and linearity are improved.

III. Measurement Results

The radiation performance of the antenna array is measured in a full anechoic chamber, and the setup is shown in Fig. 9(a) and (b). An antenna array with two concentric antenna pairs is designed with FR4. As shown in Fig. 9(a), the distance between each patch antenna is $\lambda_0/2$. Since the input outphasing signal of each concentric antenna pair is the differential signal, the patch antenna elements in the concentric antenna pair are opposite positioned. The patch antenna element operates around 2.45 GHz.

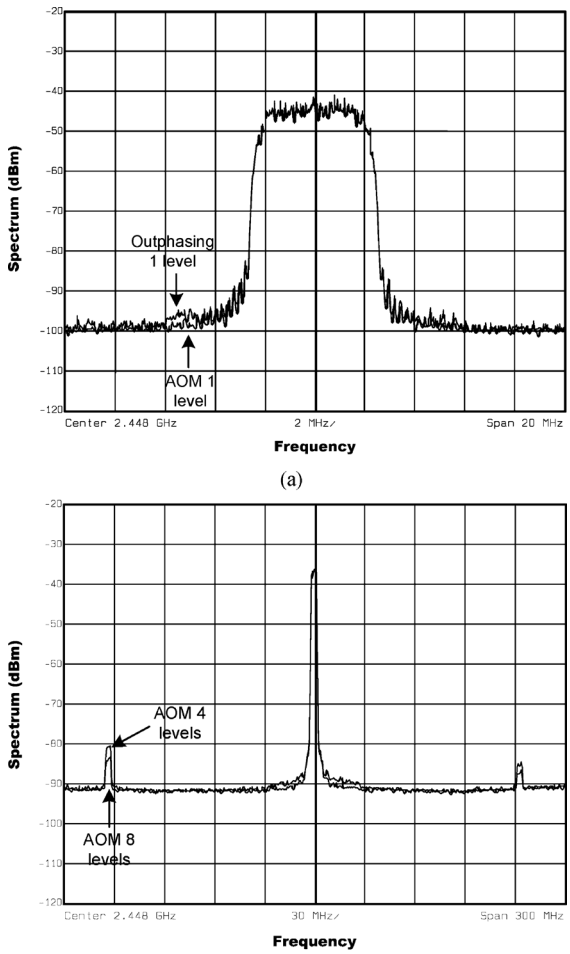

Fig. 11. E-plane $\text{azimuth} = 0°$ and $\text{elevation} = 0°$, the measured spectrum of 2.448 GHz QPSK modulation signal when applying (a) single level LINC and AOM signals. (b) 4 and 8 levels AOM signals.

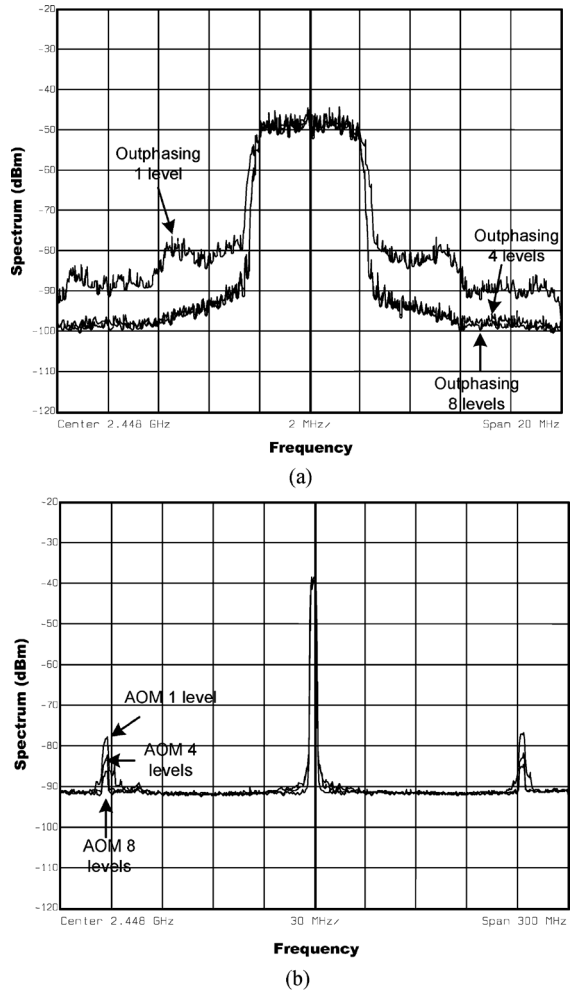

Fig. 12. E-plane $\text{azimuth} = 30°$ and $\text{elevation} = 0°$, the measured spectrum of 2.448 GHz QPSK modulation signal when applying 1, 4, and 8 levels. (a) LINC signals. (b) AOM signals.

The antenna pairs are connected to an arbitrary waveform generator that generates the differential RF signals. A horn antenna with a low noise amplifier (LNA) is connected with a spectrum analyzer to measure the received power. The radiation patterns in E-and H-planes of each concentric antenna pair are measured respectively. The results are shown in Fig. 10(a) and (b), respectively. The difference between each antenna pair represents the gain mismatch of the combined signal.

A 2.448 GHz RF signal modulated with a 3.84 Mbps QPSK signal is employed for the spatial linear modulation measurement. The single level, 4 and 8 levels of LINC and AOM signals are generated respectively with the arbitrary waveform generator. The measurement results in E-and H-planes with single level and multilevel of LINC and AOM signals are presented. Figs. 11–13 show the measured results of the 1, 4, and 8 levels of the LINC and AOM signals in E-plane $\text{elevation} = 0°$ and with $\text{azimuth} = 0°, 30°, 60°$ respectively. The same measurement results in H-plane $\text{elevation} = 0°$ and $\text{azimuth} = 0°$ are illustrated in Fig. 14. In addition, the error vector magnitude (EVM) of the spatial modulator in E-and H-planes with different angles is also measured with a vector signal analyzer (VSA). The measured results are summarized in Table I. The WCDMA EVM specification is 17.5%, and the measured results are well below it.

From the above measurement, the correct reception angle is increased and the adjacent channel interference is reduced compared with the spatial directional modulator [5]–[10], and the distortion of LINC and the mixed components of AOM can be reduced with multilevel modulation. With the help of notch filters or other specially designed band pass function antenna, the mixed components of the AOM architecture can be reduced further [20], [21].

IV. Conclusion

A novel method for RF spatial modulation and amplification has been presented, which simplifies the design of the RF transmitter for high power efficiency. Constant envelope single level or multi-level signals have been applied for the spatial modulation. It has been shown that the multi-level signals can be used to reduce the distortion of the outphasing modulation, and the level of the mixed components of AOM modulation. The configuration of concentric antenna pairs has exhibited the capability for eliminating the phase delay difference of the modu-

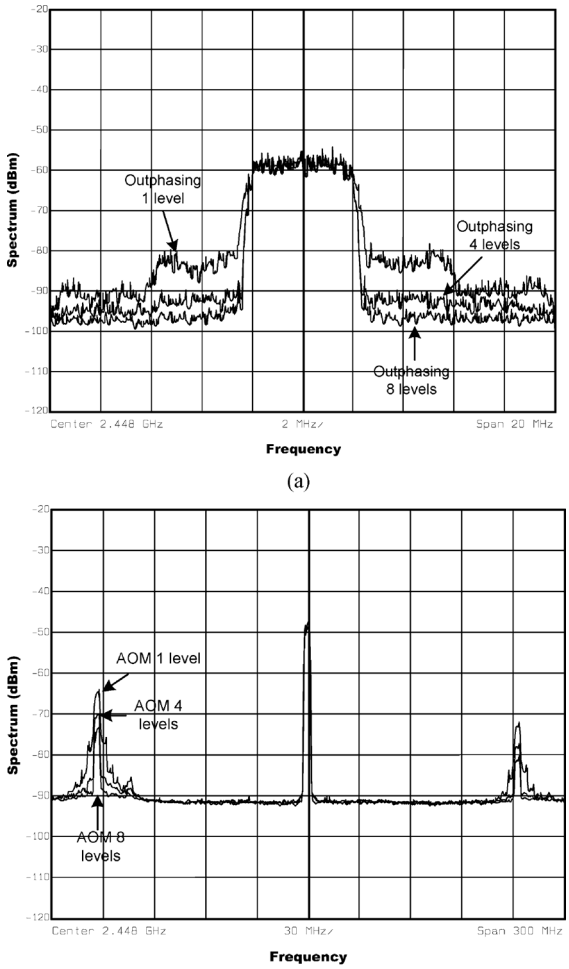

Fig. 13. E-plane azimuth $= 60°$ and elevation $= 0°$, the measured spectrum of 2.448 GHz QPSK modulation signal when applying 1, 4, and 8 levels. (a) LINC signals. (b) AOM signals.

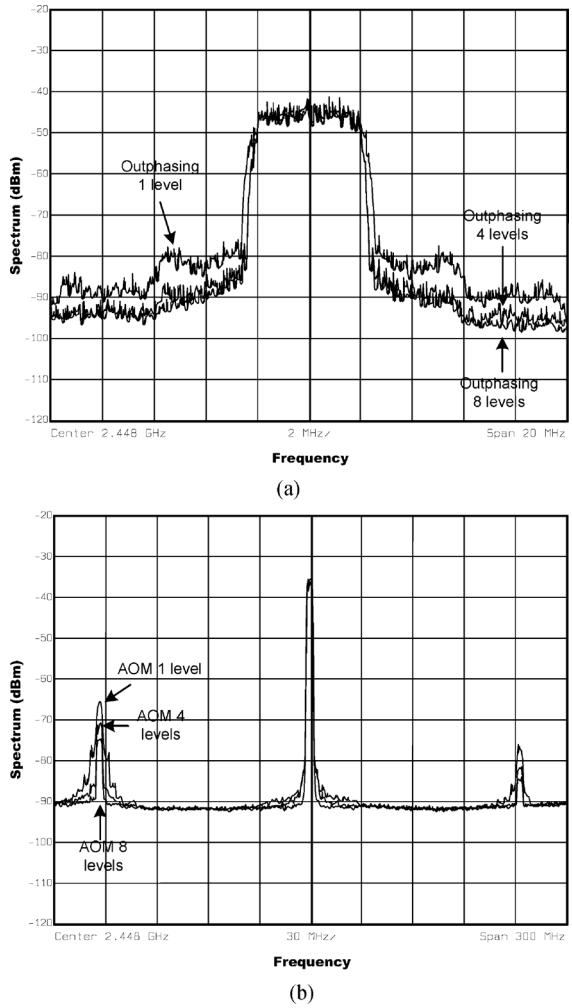

Fig. 14. H-plane azimuth $= 0°$ and elevation $= 0°$, the measured spectrum of 2.448 GHz QPSK modulation signal when applying 1, 4, and 8 levels. (a) LINC signals. (b) AOM signals.

TABLE I
SUMMARY OF THE EVM PERFORMANCE

	azimuth=0°, elevation=0°	azimuth=30°, elevation=0°	azimuth=60°, elevation=0°
E-plane Outphasing 1 level	1.07%rms	1.99%rms	4.31%rms
E-plane Outphasing 4 levels	0.77%rms	1.40%rms	2.18%rms
E-plane Outphasing 8 levels	0.89%rms	1.29%rms	1.40%rms
E-plane AOM 1 level	1.29%rms	1.36%rms	1.59%rms
E-plane AOM 4 levels	0.87%rms	0.97%rms	1.30%rms
E-plane AOM 8 levels	0.79%rms	1.04%rms	1.21%rms
H-plane Outphasing 1 level	1.81%rms	1.46%rms	9.84%rms
H-plane Outphasing 4 levels	0.98%rms	0.93%rms	4.12%rms
H-plane Outphasing 8 levels	0.83%rms	1.30%rms	2.43%rms
H-plane AOM 1 level	1.30%rms	1.20%rms	1.60%rms
H-plane AOM 4 levels	1.09%rms	1.38%rms	1.55%rms
H-plane AOM 8 levels	0.85%rms	0.75%rms	1.48%rms

lated signals from different antenna pairs, and thus minimized the distortion introduced by the mismatch of the phase delay. The proposed method is suitable for antenna-on-chip (AoC), antenna-in-package (AiP) or active integrated antenna (AIA) designs.

REFERENCES

[1] A. Valdes-Garcia *et al.*, "A fully integrated 16-element phased-array transmitter in SiGe BiCMOS for 60-GHz communications," *IEEE J. Solid State Circuits*, vol. 45, no. 12, pp. 2757–2773, Dec. 2010.

[2] A. Natarajan *et al.*, "A 77-GHz phased-array transceiver with on-chip antennas in silicon: Transmitter and local LO-path phase shifting," *IEEE J. Solid State Circuits*, vol. 41, no. 12, pp. 2807–2819, Dec. 2006.

[3] Y. A. Atesal *et al.*, "Millimeter-wave wafer-scale silicon BiCMOS power amplifiers using free-space power combining," *IEEE Trans. Microwave Theory Tech.*, vol. 59, no. 4, pp. 954–965, Apr. 2011.

[4] M. P. DeLisio and R. A. York, "Quasi-optical and spatial power combining," *IEEE Trans. Microw. Theory Tech.*, vol. 50, no. 3, pp. 929–936, Mar. 2002.

[5] A. Babakhani, D. B. Rutledge, and A. Hajimiri, "Transmitter architectures based on near-field direct antenna modulation," *IEEE J. Solid-State Circuits*, vol. 43, no. 12, pp. 2674–2692, Dec. 2008.

[6] A. Babakhani, D. B. Rutledge, and A. Hajimiri, "Near-field direct antenna modulation," *IEEE Microwave Mag.*, vol. 10, no. 1, pp. 36–46, Feb. 2009.

[7] M. P. Daly and J. T. Bernhard, "Directional modulation technique for phased arrays," *IEEE Trans. Antennas Propag.*, vol. 57, no. 9, pp. 2633–2640, Sep. 2009.

[8] M. P. Daly, E. L. Daly, and J. T. Bernhard, "Demonstration of directional modulation using a phased array," *IEEE Trans. Antennas Propag.*, vol. 58, no. 5, pp. 1545–1550, May 2010.

[9] M. P. Daly and J. T. Bernhard, "Beamsteering in pattern reconfigurable arrays using directional modulation," *IEEE Trans. Antennas Propag.*, vol. 58, no. 7, pp. 2259–2265, Jul. 2010.

[10] C. K. Liang and B. Razavi, "Transmitter linearization by beamforming," *IEEE J. Solid State Circuits*, vol. 46, no. 9, pp. 1956–1969, Sep. 2011.

[11] H. Chireix, "High power outphasing modulation," *Proc. IRE*, vol. 23, no. 11, pp. 1370–1392, Nov. 1935.
[12] D. C. Cox, "Linear amplification with nonlinear components," *IEEE Trans. Commun.*, vol. COM-22, no. 12, pp. 1942–1945, Dec. 1974.
[13] Y. Zhou and M. Y. W. Chia, "A novel alternating and outphasing modulator for wireless transmitter," *IEEE Trans. Microw. Theory Tech.*, vol. 58, no. 2, pp. 324–330, Feb. 2010.
[14] X. Zhang, L. E. Larson, and P. M. Asbeck, *Design of Linear RF Outphasing Power Amplifiers*. Norwood, MA, USA: Artech House, 2003.
[15] A. Birafane *et al.*, "Analyzing LINC systems," *IEEE Microwave Mag.*, vol. 11, no. 5, pp. 59–71, Aug. 2010.
[16] S. Gao and P. Gardner, "Integrated antenna/power combiner for LINC radio transmitters," *IEEE Trans. Microw. Theory Tech.*, vol. 53, no. 3, pp. 1083–1088, Mar. 2005.
[17] A. Birafane and A. B. Kouki, "On the linearity and efficiency of outphasing microwave amplifiers," *IEEE Trans. Microw. Theory Tech.*, vol. 52, no. 7, pp. 1702–1708, Jul. 2004.
[18] C. A. Balanis, *Antenna Theory: Analysis and Design*, 3rd ed. Hoboken, NJ, USA: Wiley, 2005.
[19] K. Y. Jheng, Y. J. Chen, and A. Y. Wu, "Multilevel LINC system designs for power efficiency enhancement of transmitters," *IEEE J. Sel. Topics Signal Process.*, vol. 3, no. 3, pp. 523–532, Jun. 2009.
[20] Y. Zhang *et al.*, "Design and implementation of planar ultra-wideband antennas with multiple notched bands based on stepped impedance resonators," *IET Microw., Antennas Propag.*, vol. 3, no. 7, pp. 1051–1059, Oct. 2009.
[21] F. Bayatpur and K. Sarabandi, "Miniaturized FSS and patch antenna array coupling for angle-independent, high-order spatial filtering," *IEEE Microw. Wireless Compon. Lett.*, vol. 20, no. 2, pp. 79–81, Feb. 2010.
[22] Mini-Circuits ZFRSC-42 Data Sheet [Online]. Available: http://www.minicircuits.com/pdfs/ZFRSC-42+.pdf

Yijun Zhou (M'03) received the B.Sc. degree in electronic engineering from Zhejiang University, Hangzhou, China, in 1987, the M.Eng. degree from the Shanghai University of Science and Technology, Shanghai, China, in 1990, and the Ph.D. degree from Lund University, Lund, Sweden, in 2003.

From 1990 to 1996, he was a Research and Development Engineer with the Zhejiang Telecommunication Equipment Factory. Since 1996, he has been with the Institute for Infocomm Research (I^2R), Agency for Science, Technology and Research, (A*STAR), Singapore, where he was a Research and Development Engineer, and since 2003, he has been a Scientist. His current research interests are mixed-signal and RF CMOS circuit design.

Michael Yan-Wah Chia (SM'05) was born in Singapore in 1966. He received the B.Sc. (First Class Honours) and the Ph.D. degrees from Loughborough University, U.K., in 1990 and 1994, respectively.

In 1994, he joined the Center for Wireless Communications (CWC), National University of Singapore (NUS), as a Member of Technical Staff. In 2003, he became the Communications Division Director in the Institute for Infocomm Research (merger of several national research centers) of Agency for Science, Technology and Research, (A*STAR) to manage four head of departments (about 200 staff in the division). Since then, he has held various corporate management appointments as a Program Director, Director-Industry, and Deputy Executive Director-Industry leading teams of program managers. He is now holding the rank of Principal Scientist II in A*STAR. Since August 2012, he has been leading a new technology program on Power Aware Transceivers. He is concurrently a Full Professor (Adjunct) at the NUS. He has also held appointments in several technical/advisory committees in industry and national government bodies. To date, he has contributed to more than 180 publications in international journals (81) and conferences (99). He has at least 14 patents granted. He has led several major wireless research programs in Singapore, particularly in the areas of RFID, UWB and Terahertz, He has also secured and led many major projects funded by industry, e.g., BOSCH, EADS, and IBM (IBM Biz Partner Program for silicon designs). His research interests are in phased array, terahertz, millimeterwave, UWB, beam-steering, RFID, antenna, transceiver, RFIC, power amplifier, linearization, wireless communication, and radar sensors.

Prof. Chia was a recipient of the Overseas Research Student (ORS) Awards from U.K. universities and the Research Studentship Award from British Aerospace, U.K. He has contributed actively to several international conferences in the organizing committees. He was the Program Co-Chair of IEEE International Workshop of Antenna Technology (IWAT) 2005, keynote speaker for the IEEE International Conference of Ultra-wideband, ICUWB 2005-Zurich, General Chair of ICUWB 2007-Singapore, and Vice Technical Program Chair in 2012 ICUWB-Syracuse. He has been a member of the Executive Committee of ICUWB since 2007. He is a member of the editorial board of the IEEE TRANSACTIONS ON MICROWAVE THEORY AND TECHNIQUES and is an editor of several international journals.

Xianming Qing (M'90) received the B.Eng. degree from the University of Electronic Science and Technology of China (UESTC) in 1985 and the Ph.D. from Chiba University, Japan, in 2010.

During 1987–1996, he was with UESTC for teaching and research and appointed as a Lecturer in 1990 and an Associate Professor in 1995. He joined National University of Singapore (NUS) in 1997 as a Research Scientist. Since 1998, he has been with the Institute for Infocomm Research (I^2R, formerly known as CWC and ICR), Singapore. He currently holds the position of Senior Scientist and the Leader of antenna group under the RF and Optical Department. His main research interests are antenna design and characterization for wireless applications. In particular, his current R&D focuses on small and broadband antennas/arrays for wireless systems, such as ultra-wideband (UWB) systems, radio frequency identification (RFID) systems and medical imaging systems, microwave, mmW, submmW, and THz imaging systems. He has authored and coauthored over 150 technical papers published in international journals or presented at international conferences, and five book chapters.

Dr. Qing has been a member of the IEEE Antennas and Propagation Society since 1990. He was the recipient of the IES Prestigious Engineering Achievement Award 2006, Singapore and the ISAP 2010 Best Paper Award. He has served as a member of the RFID Technical Committee (TC-24) of the IEEE MTT since 2009. He served as the Organizer and Chair for Special Sessions on RFID Antennas at IEEE Antenna and Propagation Symposium 2007 and 2008. He is serving as an Associate Editor of the *International Journal of Microwave and Wireless Technologies* and the *International Journal of Microwave Science and Technology*. He also served the Guest Editor of the *International Journal on Wireless & Optical Communications* Special Issue on "Antennas for Emerging Radio Frequency Identification (RFID) Applications." He has served as a TPC member and Session Chair for a number of conferences, and as a regular reviewer for the IEEE TRANSACTIONS ON ANTENNAS AND PROPAGATION, the IEEE TRANSACTIONS ON MICROWAVE THEORY AND TECHNIQUES, the IEEE ANTENNAS AND WIRELESS PROPAGATION LETTERS, the IEEE MICROWAVE AND WIRELESS COMPONENTS LETTERS,*IET-MAP, Electronic Letters*, etc. He holds ten granted and filed patents. He has received six awards of advancement of science and technology in China.

Jiren Yuan received the B.Sc. degree in radio engineering from Harbin Polytechnical University, China, in 1964, and the Licentiate degree, the Ph.D. degree, and the Docent degree in electronic devices from Linköping University, Sweden, in 1988, 1989, and 1993, respectively.

From 1989 to 1991, he was an Assistant Professor and, from 1991 to 1997, an Associate Professor at Linköping University. In September 1997, he became a Professor and joined the Department of Applied Electronics (now Electrical and Information Technology), Lund University, Sweden, chairing the Circuit Design Group. From 1998 to 2007, he was the Director of the Competence Center for Circuit Design, a VINNOVA competence center in Sweden. He retired in 2008. He has published approximately 80 papers in international journals and conferences and holds seven patents. His research interests are in the area of high-performance CMOS circuits and systems.

Prof. Yuan received the Solid-State Circuits Council 1988–1989 Best Paper Award and the Excellent Paper Award of the 6th International Conference on ASIC (ASICON 2005).